

Article

Theoretical Estimation of Energy Balance Components in Water Networks for Top-Down Approach

Surachai Lipiwattanakarn, Suparak Kaewsang, Natchapol Charuwimolkul, Jiramate Changklom and Adichai Pornprommin * 

Department of Water Resources Engineering, Faculty of Engineering, Kasetsart University, Bangkok 10900, Thailand; fengsuli@ku.ac.th (S.L.); suaparak.k@ku.th (S.K.); natchapol.ch@ku.th (N.C.); jiramate.ch@ku.th (J.C.)

* Correspondence: fengacp@ku.ac.th

Abstract: The energy balance calculation for pressurized water networks is an important step in assessing the energy efficiency of water distribution systems. However, the calculation generally requires mathematical modelling of the water networks to estimate three important energy components: outgoing energy through water loss (E_l), friction energy loss (E_f) and energy associated with water loss (E_{WL}). Based on a theoretical energy balance analysis of simplified pipe networks, a simple method is proposed to estimate E_l , E_f and E_{WL} with minimum data requirements: input energy, water loss (WL) and head loss between the source and the minimum energy point (ΔH). By inclusion of the head loss in water networks into the estimation, the percentages of E_l and E_{WL} are lower and higher, respectively, than using only the percentage of WL . The percentage of E_f can be a function of the percentage of ΔH . By demonstrating our analysis with the simulation results from the mathematical models of 20 real water networks, the proposed method can be used to effectively estimate E_l , E_f and E_{WL} as a top-down energy balance approach.

Keywords: energy balance; friction; water loss; pressurized water networks; theoretical estimation



Citation: Lipiwattanakarn, S.; Kaewsang, S.; Charuwimolkul, N.; Changklom, J.; Pornprommin, A. Theoretical Estimation of Energy Balance Components in Water Networks for Top-Down Approach. *Water* **2021**, *13*, 1011. <https://doi.org/10.3390/w13081011>

Received: 19 February 2021

Accepted: 6 April 2021

Published: 7 April 2021

Publisher's Note: MDPI stays neutral with regard to jurisdictional claims in published maps and institutional affiliations.



Copyright: © 2021 by the authors. Licensee MDPI, Basel, Switzerland. This article is an open access article distributed under the terms and conditions of the Creative Commons Attribution (CC BY) license (<https://creativecommons.org/licenses/by/4.0/>).

1. Introduction

The demand for energy is intensifying in the water sector. The International Energy Agency (IEA) [1] estimated that 4% of total global electricity was consumed by the water sector in 2014 and it may rise by 80% by 2040. In Portugal, urban water and wastewater systems use 3%–4% of the total national electricity [2]. In Brazil, over 1.9% of total electricity energy is consumed by water supply systems [3]. Pelli and Hitz [4] estimated that supplying drinking water and industrial water worldwide can consume as much as 2%–10% of a country's total electricity usage. The World Bank [5] reported that electricity costs are 5%–30% of the total operating cost of water and wastewater utilities worldwide. In Latin America and the Caribbean, energy is generally 30%–40% of the operational costs of water supply services [6]. Nevertheless, IEA [1] suggested that there is a great opportunity to save energy in the water sector by 15% by 2040 if economically available energy efficiency and energy recovery potentials are exploited. Achieving this will require accurate and comprehensive energy assessment in the water sector.

In the past, energy assessment in water supply systems was focused on pump inefficiency. Later, the interest extended to assess the energy losses due to friction and leakage in water networks [4,7,8]. Bylka and Mroz [9] reviewed energy assessment methods for water supply systems and categorized them into two groups. While the first group is based solely on data collected in water utilities, the second one is based on both the data and modelling of physical processes. Thus, more detailed results from the second group can support a strategy for increasing the energy efficiency of each process. Since mathematical modelling requires collecting a large amount of data and is time consuming to analyze, it is usually applied on a relatively small network. Cabrera et al. [10] presented one of the first energy audit methods for water networks based on the modelling of physical processes. Over the

past decade, more complex and comprehensive methods have been developed for energy balance and assessment based on physical processes to evaluate energy transformation and efficiency in water supply systems [11–22]. In addition, there are successful energy assessments of real networks based on physical processes in many countries [19–27].

Figure 1 shows two simplified versions of energy balances in water networks considering only leakage (as water loss) and pipe friction proposed by Cabrera et al. [10] and Mamade et al. [19–21]. The energy balance in Cabrera et al. [10] (Figure 1a) shows the input energy (E_{in}) divided into three components: the energy delivered to users (E_u), the outgoing energy through water loss (E_l) and the friction energy loss (E_f). To be consistent with the International Water Association (IWA) water balance [28], on the other hand, Mamade et al. [19–21] divided E_{in} into two components: the energy associated with authorized consumption (E_{AC}) and the energy associated with water loss (E_{WL}), as shown in Figure 1b. Theoretically, these components should be calculated through mathematical models, which are based on physical processes. For the balance in Cabrera et al. [10], a calibrated mathematical model is sufficient to evaluate E_u , E_l and E_f . However, for the balance in Mamade et al. [19–21], an additional model without water loss is needed to estimate the friction energy loss for a water loss-free network (E_{fo}). Mamade et al. [21] proposed the top-down and bottom-up approaches for their energy balance. In the top-down approach, the ratio between E_{WL} and E_{in} is assumed to be the ratio between water loss (WL) and system input volume (SIV). To prove the assumption, the comparison between E_{WL}/E_{in} and WL/SIV was carried out through simulation using the mathematical models of real networks. The linear trendline shows that the value E_{WL}/E_{in} is slightly higher than WL/SIV . In this study, the evaluation of E_{WL}/E_{in} is reanalyzed by using both theoretical analysis and mathematical models and the estimations of E_l/E_{in} and E_f/E_{in} are also investigated. In Section 2, the theoretical analysis of energy balance describes the behaviors of each energy balance component and establishes the basic relationships between each variable. In Section 3, the mathematical models of 20 real district metering area (DMA) networks are introduced, and the relationships between the model results and basic parameters are investigated. Section 4 combines the results from the theory and the models, and the coefficient in the theory is calibrated using the model simulation results. The accuracy of the estimation of E_l , E_f and E_{WL} is evaluated in order to apply as the top-down energy balance approach. Finally, the conclusion is provided in Section 5.

Input energy (E_{in})	Energy delivered to users (E_u)	Input energy (E_{in})	Energy associated with au- thorized consumption ($E_{AC} = E_u + E_{fo}$)
	Outgoing energy through water loss (E_l)		Energy associated with wa- ter loss ($E_{WL} = E_l + E_f - E_{fo}$)
	Friction energy loss (E_f)		

(a)

(b)

Figure 1. Two simplified energy balance concepts in water networks considering only leakage (as water loss) and pipe friction, where (a) is proposed by Cabrera et al. [10] and (b) is proposed by Mamade et al. [19–21].

2. Theoretical Analysis of Energy Balance

In this section, the energy balance principle is introduced and analyzed theoretically on two simple pressurized water networks. The energy balance components are calculated and then normalized to the non-dimensional version. They are used for the top-down energy balance estimation.

2.1. Single Pipe Network

As the first case, Figure 2 shows a single pipe network consisting of a source and a demand node at the pipe end. The input energy head is defined as H , and the system inflow is Q . Using the water balance concept, Q can be divided into

$$Q = Q_u + Q_l \quad (1)$$

where Q_u is the flow to supply authorized consumption and Q_l is the flow due to water loss. Then, we introduce the ratio of water loss (p) as

$$p = \frac{Q_l}{Q} \quad (2)$$

At the demand node at the pipe end, Q is out of the network and thus, the friction head loss along the pipe (ΔH) can be expressed as

$$\Delta H = KQ^n \quad (3)$$

where K is the loss coefficient and n is the flow exponent.

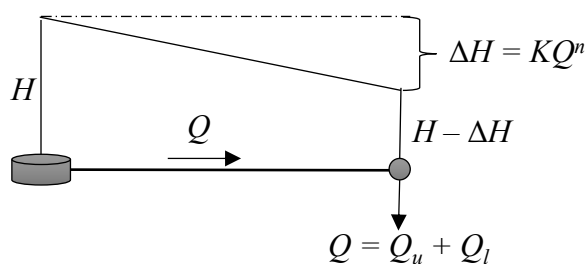


Figure 2. Energy balance for single pipe network.

According to the energy balance concepts in Figure 1, the energy balance components can be calculated as

1. Input energy (E_{in})

$$E_{in} = \gamma QH \quad (4)$$

2. Outgoing energy through water loss (E_l)

$$E_l = \gamma Q_l (H - KQ^n) \quad (5)$$

3. Friction energy loss (E_f)

$$E_f = \gamma Q (KQ^n) \quad (6)$$

4. Friction energy loss for a water loss-free network (E_{fo})

$$E_{fo} = \gamma Q_u (KQ_u^n) \quad (7)$$

5. Energy associated with water loss (E_{WL})

$$E_{WL} = E_l + E_f - E_{fo} \quad (8)$$

where γ is specific weight of water.

The nondimensionalization is introduced here. According to Mamade et al. [21], E_{WL} divided by E_{in} can be approximated by p . Therefore, the energy balance components in Equations (4)–(8) are normalized by E_{in} as

$$\left(E'_{in}, E'_l, E'_f, E'_{fo}, E'_{WL}\right) = \frac{\left(E_{in}, E_l, E_f, E_{fo}, E_{WL}\right)}{E_{in}} \quad (9a)$$

and ΔH is normalized by H as

$$\Delta H' = \frac{KQ^n}{H} = \frac{\Delta H}{H} \quad (9b)$$

where the variables with superscript ' are the normalized versions of the variables.

Thus, the normalized energy balance components for the first case in Figure 2 can be written as

1. Normalized input energy (E'_{in})

$$E'_{in} = 1 \quad (10)$$

2. Normalized outgoing energy through water loss (E'_l)

$$E'_l = \left(\frac{Q_l}{Q}\right) \left(\frac{H - KQ^n}{H}\right) = p - p\Delta H' \quad (11)$$

3. Normalized friction energy loss (E'_f)

$$E'_f = \Delta H' \quad (12)$$

4. Normalized friction energy loss for a water loss-free network (E'_{fo})

$$E'_{fo} = \left(\frac{Q_u}{Q}\right) \left(\frac{KQ_u^n}{H}\right) = (1 - p)^{n+1} \Delta H' \quad (13)$$

5. Normalized energy associated with water loss (E'_{WL})

$$E'_{WL} = p + p_n \Delta H' \quad (14)$$

where

$$p_n = (1 - p)[1 - (1 - p)^n] \quad (15)$$

The energy components relating to water loss, E'_l and E'_{WL} in Equations (11) and (14), have a linear relationship with p only if $\Delta H'$ is null. Thus, the hypothesis of Mamade et al. [21] is valid under the no energy loss condition. Both E'_l and E'_{WL} depend on $\Delta H'$ in Equation (9b). The value of $\Delta H'$ should be between 0 and 1. If the head loss (ΔH) is sufficiently smaller than the input head (H), $\Delta H'$ will be close to 0. As a result, E'_l is slightly smaller than p , while E'_{WL} is slightly larger than p . On the other hand, if ΔH is comparable to H , $\Delta H'$ will approach unity, and the discrepancies between E'_l , E'_{WL} and p grow with an increase in $\Delta H'$. Figure 3 shows p_n as a function of p from Equation (15) for $n = 1, 1.852$ and 2 . If $n = 1$, it implies a laminar flow, and the curve is a negative parabola with the maximum p_n of 0.25 at $p = 0.5$ and the minimum p_n of 0 at $p = 0$ and 1. For the case of complete turbulence, rough pipes ($n = 2$), the curve is skewed to the right with the maximum p_n of around 0.385 at $p \approx 0.423$. For the Hazen–Williams formula ($n = 1.852$), the curve differs from the $n = 2$ curve slightly. Thus, E'_{WL} approaches p when p is very low or extremely high, and the maximum deviation of E'_{WL} from p occurs when the percentage of water loss is around 40%–50%. In this study, n is assumed to be 2 for simplicity.

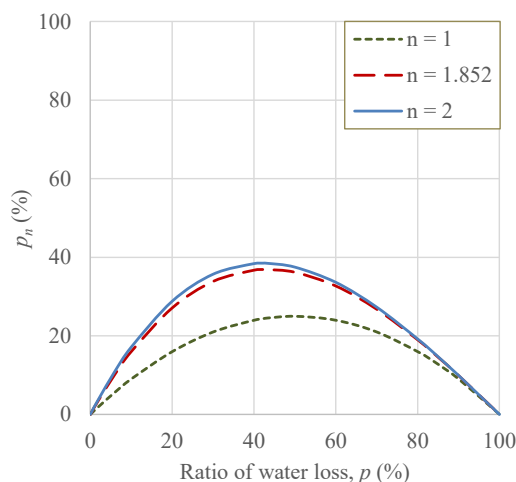


Figure 3. Relationship between parameter p_n and ratio of water loss, p .

2.2. Branched Pipe Network with Uniformly Distributed Demand Nodes

The effects of branching and demand distribution on energy balance are investigated theoretically in this section. Here, the second network is introduced. It consists of branched pipes, and each branched pipe has uniformly distributed demand nodes as shown in Figure 4. A parameter m denotes the number of branches, and j denotes the number of demand nodes in each branch. Each branch has the same hydraulic properties, where the demand nodes have the same outflow of $Q/m/j$ and they distribute uniformly along the branch. In addition, the constant friction slope along each branch is assumed, and the head loss equals $K(Q/m)^n$ at the end of each branch. These assumptions are used to simplify the problem and to make it possible to be solved theoretically. They will be discussed in the later section using the results from the real network models.

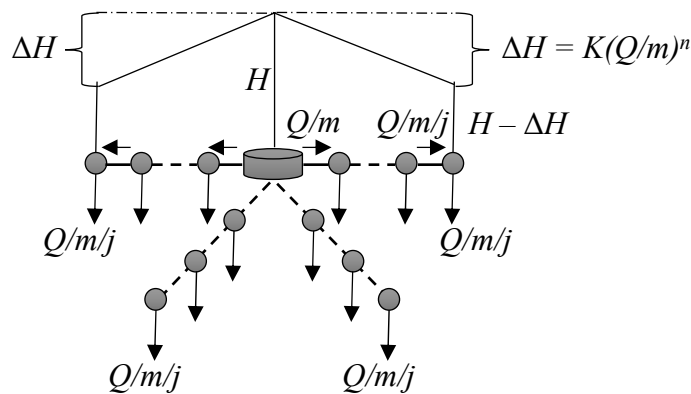


Figure 4. Energy balance for simplified branched pipe network with uniformly distributed demand nodes, where m is number of branches and j is number of demand nodes in each branch.

For the network in Figure 4, the energy balance components can be calculated as follows.

1. Input energy (E_{in})

$$E_{in} = \gamma QH \tag{16}$$

2. Outgoing energy through water loss (E_l)

$$E_l = m \sum_{i=1}^j \gamma \frac{Q_{li}}{m} \left[H - \frac{i}{j} K \left(\frac{Q}{m} \right)^n \right] = \gamma Q_l \left[H - \left(\frac{1}{2m^n} \right) \left(1 + \frac{1}{j} \right) K Q^n \right] \tag{17}$$

3. Friction energy loss (E_f)

$$E_f = m \sum_{i=1}^j \gamma \frac{Q_i}{m} \frac{K \left(\frac{Q_i}{m} \right)^n}{j} = \left(1 + \frac{1}{j} \right) \frac{\gamma Q (KQ^n)}{2m^n} \quad (18)$$

4. Friction energy loss for a water loss-free network (E_{fo})

$$E_{fo} = \left(1 + \frac{1}{j} \right) \frac{\gamma Q_u (KQ_u^n)}{2m^n} \quad (19)$$

5. Energy associated with water loss (E_{WL})

$$E_{WL} = E_l + E_f - E_{fo} \quad (20)$$

Using the nondimensionalization in Equation (9a,b) the normalized energy balance components can be written as

1. Normalized input energy (E'_{in})

$$E'_{in} = 1 \quad (21)$$

2. Normalized outgoing energy through water loss (E'_l)

$$E'_l = p - C_{mj} p \Delta H' \quad (22)$$

3. Normalized friction energy loss (E'_f)

$$E'_f = C_{mj} \Delta H' \quad (23)$$

4. Normalized friction energy loss for a water loss-free network (E'_{fo})

$$E'_{fo} = C_{mj} (1 - p)^{n+1} \Delta H' \quad (24)$$

5. Normalized energy associated with water loss (E'_{WL})

$$E'_{WL} = p + C_{mj} p_n \Delta H' \quad (25)$$

where

$$C_{mj} = \left(\frac{1}{2m^n} \right) \left(1 + \frac{1}{j} \right) \quad (26)$$

The normalized energy balance components in Equations (22)–(25) of the second case are the generalized versions of the results from the first case in Equations (11)–(14), respectively, considering the effects of branching and demand distribution on the energy balance. The parameter C_{mj} in Equation (26) is a multiplier in the $\Delta H'$ term and has a value between 0 and 1. For the network with one branch ($m = 1$) and one demand node ($j = 1$), C_{mj} equals to 1 and the components in Equations (22)–(25) are simplified into Equations (11)–(14), respectively. An increase in branches ($m > 1$) and demand nodes ($j > 1$) produces a smaller value of C_{mj} and subsequently, an increase in E'_l but a decrease in E'_f , E'_{fo} and E'_{WL} . Thus, C_{mj} is the coefficient representing different water distribution patterns. Since C_{mj} in Equation (26) is derived theoretically under many assumptions, we are going to find appropriate values of C_{mj} for each energy balance component using the results of our network models later.

2.3. Utilization of Theory to Real Networks

The estimations of three normalized energy balance components, E'_l , E'_f and E'_{WL} , for real networks are discussed here. Up to this point, our theoretical analysis considers the energy balance of a single time period. To apply the theory to a real application, the extended period analysis is performed to evaluate the time-averaged values of E'_l , E'_f and E'_{WL} . However, the time-averaged $\Delta H'$ terms may be too complicated for a top-down approach. Thus, for simplicity, we proposed the following theoretical estimations for real networks.

$$E'_{l,theo} = \bar{p} - C_{mj} \overline{p \Delta H'} \cong p - C_{mj} p \Delta H^* \quad (27)$$

$$E'_{f,theo} = C_{mj} \overline{\Delta H'} \cong C_{mj} \Delta H^* \quad (28)$$

$$E'_{WL,theo} = \bar{p} + C_{mj} \overline{p_n \Delta H'} \cong p + C_{mj} p_n \Delta H^* \quad (29)$$

where the subscript *theo* denotes the theoretical estimation, the bar $\bar{}$ expresses time average and ΔH^* is the renormalized head loss, written as

$$\Delta H^* = \frac{\bar{H}_{\max} - \bar{H}_{\min}}{\bar{H}_{\max}} \quad (30)$$

where \bar{H}_{\max} is the maximum time-averaged energy head and \bar{H}_{\min} is the minimum time-averaged energy head. The source with the maximum head can be chosen as the \bar{H}_{\max} point, and the location where the maximum head loss occurs is the \bar{H}_{\min} point. Thus, the \bar{H}_{\min} location depends on network topology as well as demand distribution. The highest possibility is the furthest dead end from the source.

3. Application to Real Water Networks

3.1. Characteristics of Water Networks

In this section, 20 real water networks (Table 1) are used to test our theoretical analysis of energy balance. They are real district metering areas (DMAs) in the service area of the Samut Prakan branch office of the Metropolitan Waterworks Authority (MWA), Thailand. Samut Prakan is a province located at the mouth of the Chao Phraya River. Thus, the elevations refer to mean sea level (MSL). While the first 10 DMAs have 1 inlet (district meter), the remaining 10 DMAs have 2 inlets. The number of customers ranges from 739 to 11,545 connections with an average of 3508 connections. The average length and distribution pipe diameter are 40.8 km and 159 mm, respectively. While the average friction slope (S_f) from our network models ranges from 0.07 m/km to 0.70 m/km with an average of 0.23 m/km, S_f from the study of Mamade et al. [21] ranges from 0.1 m/km to 1.2 m/km with an average of 0.19 m/km. Based on the average value, the networks in our study have larger values of S_f . Mamade et al. [21] explained that their networks are overdesigned; thus, the impact on head loss by adding water loss is small. This implies that the estimation of the normalized energy associated with water loss (E'_{WL}) is not sensitive to head loss in their study. However, using our theory, $E'_{WL,theo}$ in Equation (29) is a function of the normalized water loss (p) and head loss (ΔH^*), not S_f . Our case study covers values of p between 2.8% and 54.9%, and values of ΔH^* between 7.6% and 65.3%. Thus, the impact of head loss on the estimation of energy balance components can be investigated in our study.

Table 1. Characteristics of district metering areas.

ID	No. of Inlets	No. of Customers	Length	Avg. D	Avg. S_f	Water Loss, p	ΔH^*
			(km)	(mm)	(m/km)	(%)	(%)
1	1	2669	24.5	161	0.17	37.1	16.6
2	1	2657	26.4	147	0.17	28.6	35.7
3	1	4399	52.3	148	0.08	44.6	14.1
4	1	2626	46.4	174	0.20	38.5	44.2
5	1	3594	54.7	139	0.11	44.2	18.4
6	1	4812	51.0	143	0.36	54.9	40.7
7	1	4607	43.2	130	0.17	32.4	44.8
8	1	1695	28.8	208	0.09	12.9	13.7
9	1	3634	18.1	183	0.16	29.7	14.4
10	1	1820	22.5	132	0.14	2.8	14.8
11	2	1921	22.2	166	0.50	30.0	35.0
12	2	2151	19.0	154	0.16	50.9	7.6
13	2	2297	24.9	154	0.22	31.9	25.9
14	2	739	17.3	191	0.33	33.9	32.0
15	2	1468	15.9	178	0.70	7.7	34.8
16	2	4204	47.4	153	0.48	36.3	37.0
17	2	11,545	129.6	150	0.14	30.7	45.3
18	2	4460	73.7	180	0.15	30.0	65.3
19	2	4957	51.5	143	0.07	31.2	18.4
20	2	3897	47.4	154	0.28	47.2	27.8
Avg.	1.5	3508	40.8	159	0.23	32.8	29.3

Our pipe networks are modeled using the EPANET version 2.00.12.01 software (United States Environmental Protection Agency (US EPA), Columbus, OH, USA) [29]. Each customer is connected to distribution pipes by creating imaginary valves with no friction loss (not considering the friction loss on the service connection). Water loss is assumed to be pressure-dependent and simulated using the emitter function in the EPANET software. The emitter coefficients are distributed to all nodes of the networks. These extended period simulation (EPS) models are calibrated and provided by MWA and simulated on the average of the hourly base using the flow and pressure measurements and monthly water sales in March 2019. Thus, the models provide high levels of detail and accuracy. As examples, Figure 5 shows four DMAs (ID1, ID2, ID11 and ID13) used in this study, where the water distribution patterns of our networks vary from branching to semi-gridiron.

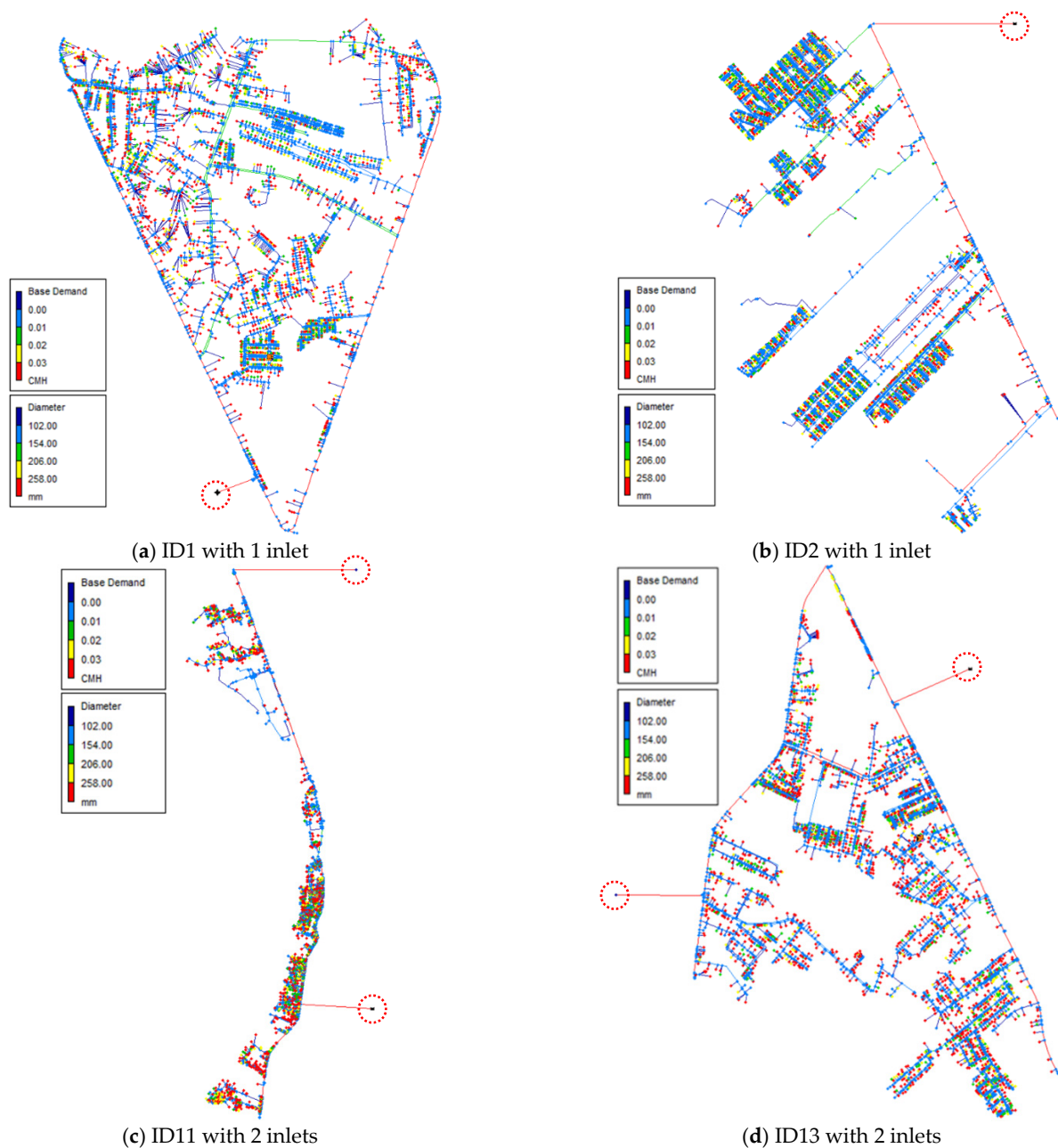


Figure 5. Examples of water networks, where (a,b) are networks with 1 inlet, and (c,d) are networks with 2 inlets. Red dashed circles show the inlets connecting to the networks by imaginary valves with no friction loss.

3.2. Basic Relationship for Energy Balance Components

The energy balance components extracted from the simulation results using EPANET (United States Environmental Protection Agency (US EPA), Columbus, OH, USA) models of 20 water networks are compared with the basic network parameters (p and ΔH^*) in Figure 6. The normalized outgoing energy through water loss by the models ($E'_{l,mod}$) shows a good relationship with p (Figure 6a). The values of $E'_{l,mod}$ are slightly to moderately smaller than p . This tendency corresponds with the estimation of $E'_{l,theo}$ in Equation (27) by our theoretical analysis, showing that $E'_{l,theo}$ is smaller than p due to the second term that relates to ΔH^* . Figure 6b shows a good relationship between the normalized friction energy loss by the models ($E'_{f,mod}$) and ΔH^* . While $E'_{f,mod}$ for 1 inlet is comparable to ΔH^* , $E'_{f,mod}$ for 2 inlets seems to be smaller than ΔH^* . According to Equation (28), $E'_{f,theo}$

depends on only ΔH^* with C_{mj} as the slope. We hypothesize that the number of inlets affects the value of C_{mj} . Thus, the calibration process of C_{mj} in the next section will divide into two groups as 1 inlet and 2 inlets. In Figure 6c, the normalized energy loss associated with water loss by the models ($E'_{WL,mod}$) shows a good relationship with p , similar to the case of $E'_{l,mod}$ in Figure 6a. However, the values of $E'_{WL,mod}$ are slightly to moderately larger than p . The result agrees with the theoretical $E'_{WL,theo}$ in Equation (29) that $E'_{WL,theo}$ is higher than p because of the additional friction energy due to an increased flow by water loss. The effect increases as ΔH^* increases.

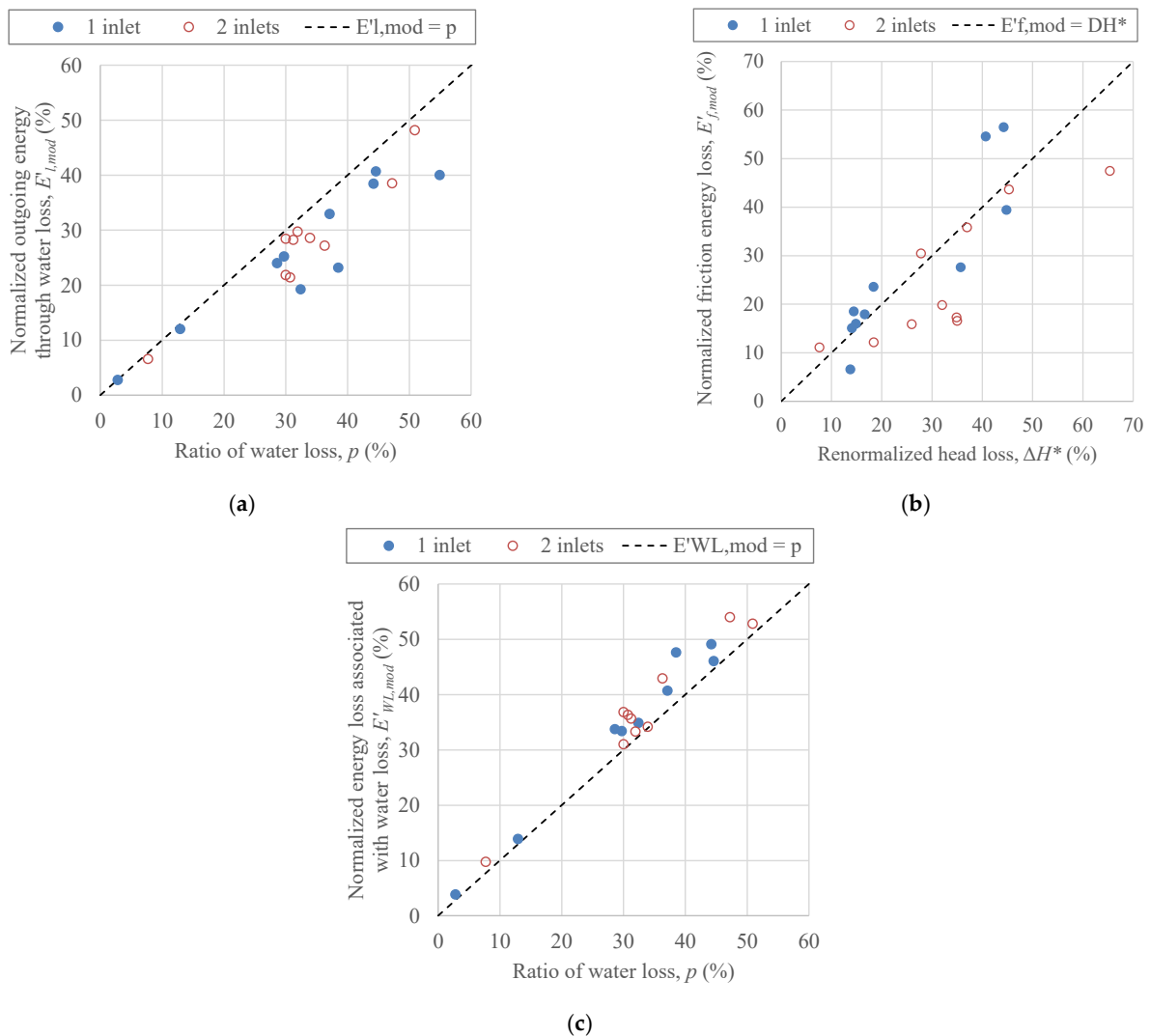


Figure 6. Relationships between energy balance components calculated by EPANET models and basic network parameters, where (a) $E'_{l,mod}$ vs. p , (b) $E'_{f,mod}$ vs. ΔH^* and (c) $E'_{WL,mod}$ vs. p .

4. Estimation of Energy Balance Components

In this section, the theoretical estimations of the energy balance components ($E'_{l,theo}$, $E'_{f,theo}$ and $E'_{WL,theo}$ in Equations (27)–(29)) are compared with the model results. Using the method of least squares, the values of the coefficient C_{mj} are evaluated separately for each energy balance component and the number of inlets. Figure 7 shows the comparisons between the three energy balance components using the EPANET models and the theoretical estimations. Table 2 shows the values of the calibrated C_{mj} used for Figure 7. In the table, “Before” means the basic relationship case that E'_l and E'_{WL} are estimated to be p and E'_f equals to ΔH^* . This case corresponds to the results in Figure 6. “After” refers to the

theoretical estimations after considering the calibrated C_{mj} in Figure 7. The correlation (r) and the root mean square error (RMSE) for the “Before” and “After” cases are evaluated. The agreements improve substantially as the terms of ΔH^* with the calibrated C_{mj} are considered. E'_l and E'_{WL} can be estimated accurately as their RMSEs are around 2%. It is possible to estimate E'_f roughly as its RMSE is around 7%. An increase in the number of inlets from 1 to 2 causes a decrease in C_{mj} , implying that the effects of branching and demand distribution become stronger. Although a number of assumptions have been used, the statistical evaluation in Table 2 shows a good performance of our theory over a wide range of p and ΔH^* . Thus, our theoretical method can be used as an effective tool to estimate the energy balance components as a top-down energy balance approach.

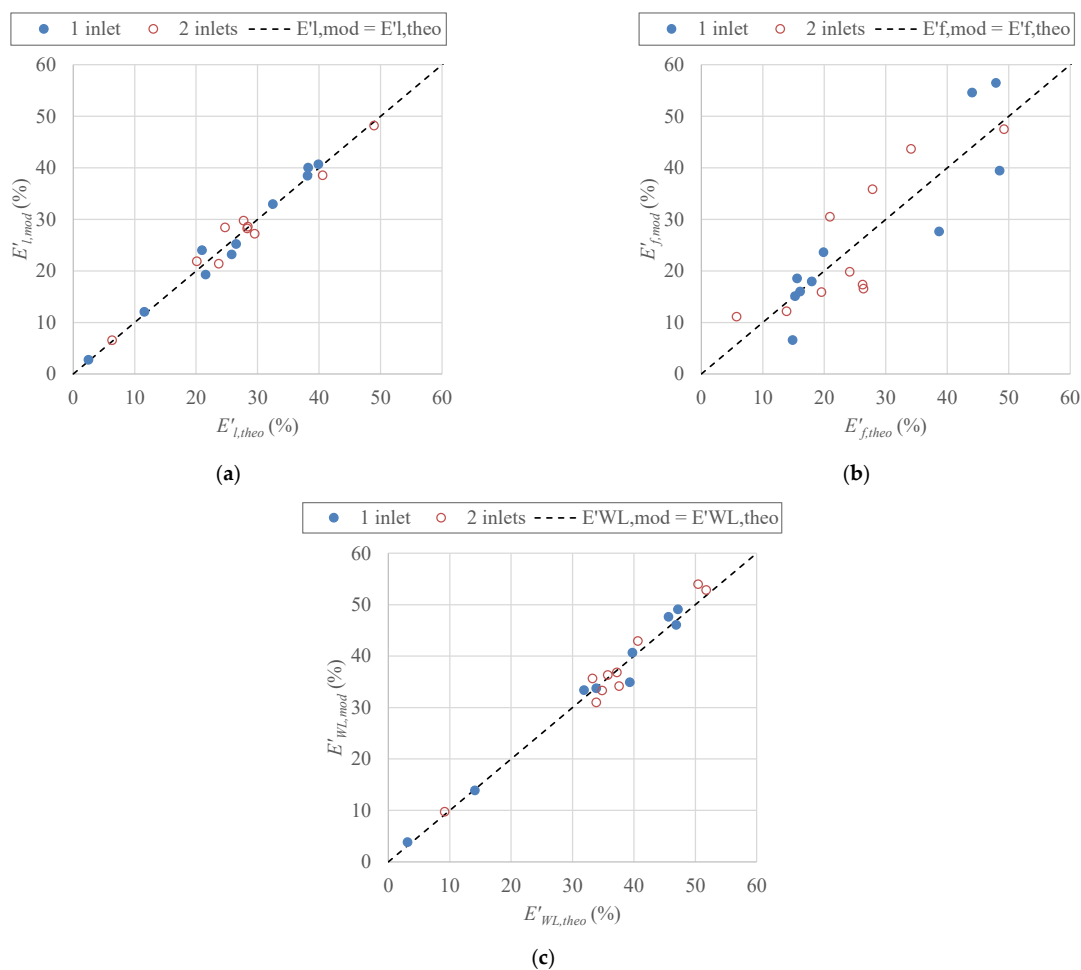


Figure 7. Comparison between energy balance components calculated by EPANET models and ones estimated by theory, where (a) $E'_{l,mod}$ vs. $E'_{l,theo}$, (b) $E'_{f,mod}$ vs. $E'_{f,theo}$ and (c) $E'_{WL,mod}$ vs. $E'_{WL,theo}$.

Table 2. Performance of proposed theoretical methods to evaluate energy balance components before and after considering normalized head loss $\Delta H'$ with calibrated coefficient C_{mj} .

Component	Equation	No. of Inlets	Value of C_{mj}	r		RMSE (%)	
				Before	After	Before	After
E'_l	(27)	1	0.7466	0.939	0.990	8.57	1.65
		2	0.5047	0.957	0.985	6.02	1.91
E'_f	(28)	1	1.0833	0.905	0.905	7.32	6.92
		2	0.7538	0.834	0.834	11.30	6.99
E'_{WL}	(29)	1	0.4219	0.992	0.994	4.75	1.83
		2	0.3095	0.978	0.984	4.46	2.17

Figure 8 shows the boxplots of the distribution of water demand in the network subarea corresponding to the head loss distribution. We cluster demand nodes of the network into 10 subareas according to the ratio of the head loss in each subarea to the total head loss ($\Delta H_i/\Delta H$) as 0.1, 0.2, . . . , 1. For example, the subarea of $\Delta H_i/\Delta H = 0.1$ means the subarea covering the demand nodes having head loss between 0%–10% of the total head loss, and the subarea of $\Delta H_i/\Delta H = 0.2$ means the one with head loss between 10%–20% of the total head loss. Then, the water demands including water loss of all nodes in each subarea are summarized and normalized by the total water demand (Q_i/Q_{in}). In our theory, the uniform distribution of water demand is assumed; thus, Q_i/Q_{in} must be constant. Under this assumption, Q_i/Q_{in} should equal to 0.1 for every subarea in this example. However, for the networks with 1 inlet in Figure 8a, more Q_i/Q_{in} is distributed in the subareas with higher $\Delta H_i/\Delta H$, implying that larger water demand is located further from the source in the energy sense. This nonuniform distribution of the demand amplifies the effect of head loss on the energy balance components. For the networks with 2 inlets, Q_i/Q_{in} is distributed in the subareas with smaller $\Delta H_i/\Delta H$ to a greater extent than for the case of 1 inlet. Thus, the effect of head loss on the energy balance components is less, as the values of C_{mj} for 2 inlets are smaller than the ones for 1 inlet in Table 2.

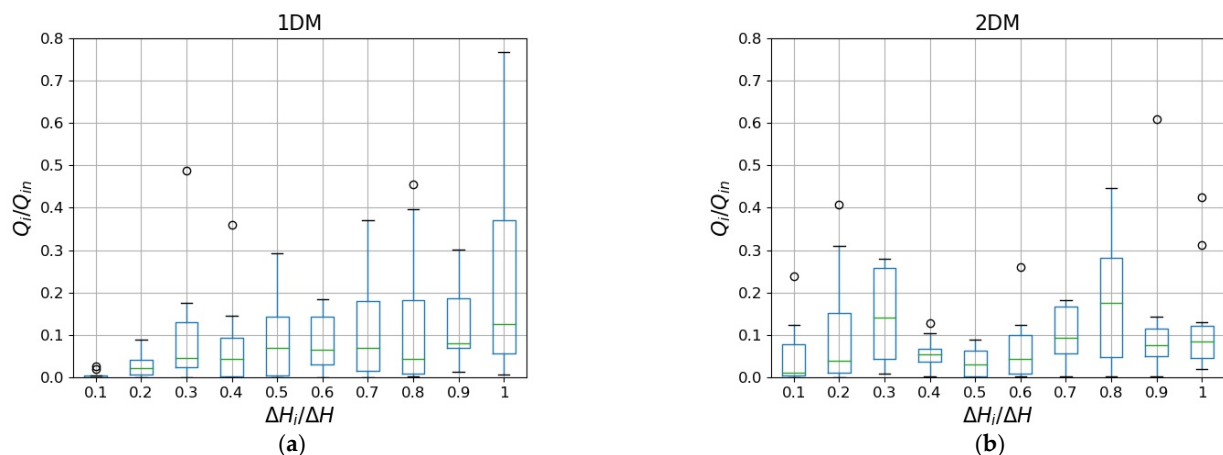


Figure 8. Boxplots of normalized demand distribution (Q_i/Q_{in}) vs. normalized head loss distribution ($\Delta H_i/\Delta H$), where (a) is for networks with 1 inlet and (b) is for networks with 2 inlets. Circles show the outliers.

5. Conclusions

To perform the energy audit based on physical processes without mathematical modelling (top-down approach), the normalized energy loss associated with water loss by the input energy (E'_{WL}) was simply assumed to equal the water loss ratio (p) as in previous studies [19–21]. Using the theoretical analysis of energy balance, the renormalized head loss by the input head (ΔH^*) was another important parameter to estimate E'_{WL} accurately. For a practical application, ΔH^* can be calculated by measuring maximum and minimum energy heads in a network. In addition, the normalized outgoing energy through water loss (E'_l) and the normalized friction energy loss (E'_f) were first derived theoretically. These energy components are fundamental and crucial for an accurate energy assessment. The effects of demand distribution in the networks with 1 and 2 inlets on the estimation of energy balance components showed that the greater number of inlets caused less head loss effects on the energy balance components. These effects can be evaluated effectively through the coefficient C_{mj} in our theory.

Author Contributions: Conceptualization, S.L. and A.P.; methodology, A.P.; software, S.L., S.K., N.C., J.C. and A.P.; validation, S.L., S.K. and A.P.; formal analysis and investigation, S.K., N.C. and A.P.; writing—original draft preparation, A.P.; writing—review and editing, S.L., J.C. and A.P.;

visualization, N.C. and A.P.; supervision, S.L., J.C. and A.P.; funding acquisition, A.P. All authors have read and agreed to the published version of the manuscript.

Funding: This research was funded by the MWA Waterworks Institute of Thailand (MWAIT), grant number 109/2561. S.K. was supported by the Ph.D. scholarship by the Faculty of Engineering, Kasetsart University, grant number 61/01/WE/D.ENG.

Institutional Review Board Statement: Not applicable.

Informed Consent Statement: Not applicable.

Data Availability Statement: Data was provided from Metropolitan Waterworks Authority, Thailand (MWA). Direct requests for these materials may be made to the provider, as indicated in the acknowledgments.

Acknowledgments: The authors would like to thank three anonymous reviewers for their constructive reviews that helped to improve the manuscript greatly. In addition, the authors gratefully acknowledge Metropolitan Waterworks Authority (MWA) for providing data sets using in this study.

Conflicts of Interest: The authors declare no conflict of interest.

Abbreviations

The following symbols are used in this paper:

DMA	district metering area
IWA	International Water Association
MWA	Metropolitan Waterworks Authority, Thailand
C_{mj}	parameter in Equation (26)
D	pipe diameter
E_{AC}	energy associated with authorized consumption
E_f	friction energy loss
E'_f	normalized friction energy loss
$E'_{f,mod}$	normalized friction energy loss evaluated by mathematical model
$E'_{f,theo}$	normalized friction energy loss estimated by theory
E_{fo}	friction energy loss for a water loss-free network
E'_{fo}	normalized friction energy loss for a water loss-free network
E_{in}	input energy
E'_{in}	normalized input energy
E_l	outgoing energy through water loss
E'_l	normalized outgoing energy through water loss
$E'_{l,mod}$	normalized outgoing energy through water loss by mathematical model
$E'_{l,theo}$	normalized outgoing energy through water loss by theory
E_{WL}	energy associated with water loss
E'_{WL}	normalized energy associated with water loss
$E'_{WL,mod}$	normalized energy associated with water loss by mathematical model
$E'_{WL,theo}$	normalized energy associated with water loss by theory
H	input energy head
j	number of demand nodes in each branch
K	loss coefficient
m	number of branches
n	flow exponent in head loss formula
p	ratio of water loss
p_n	coefficient as a function of p
Q	inflow
Q_i	flow in subarea i
Q_l	flow due to water loss
Q_u	flow to supply authorized consumption
S_f	friction slope
SIV	system input volume
WL	water loss
γ	specific gravity

ΔH	head loss between the source and the minimum energy point
$\Delta H'$	normalized head loss between the source and the minimum energy point
ΔH^*	renormalized head loss in Equation (30)
ΔH_i	head loss in subarea i

References

- International Energy Agency (IEA). *Water Energy Nexus-Excerpt from the World Energy Outlook 2016*; World Energy Outlook; IEA: Paris, France, 2016; p. 60.
- Loureiro, D.; Silva, C.; Cardoso, M.A.; Mamade, A.; Alegre, H.; Rosa, M.J. The Development of a Framework for Assessing the Energy Efficiency in Urban Water Systems and Its Demonstration in the Portuguese Water Sector. *Water* **2020**, *12*, 134. [[CrossRef](#)]
- Vilanova, M.R.N.; Balestieri, J.A.P. Exploring the water-energy nexus in Brazil: The electricity use for water supply. *Energy* **2015**, *85*, 415–432. [[CrossRef](#)]
- Pelli, T.; Hitz, H. Energy indicators and savings in water supply. *J. Am. Water Work. Assoc.* **2000**, *92*, 55–62. [[CrossRef](#)]
- World Bank. *A Primer on Energy Efficiency for Municipal Water and Wastewater Utilities*; Technical Report; 001.12. 2012b; ESMAP: Washington, DC, USA, 2012.
- WWAP. *The United Nations World Water Development Report 2014: Water and Energy*; UNESCO: Paris, France, 2014; Volume 1.
- Colombo, A.F.; Karney, B.W. Energy and Costs of Leaky Pipes: Toward Comprehensive Picture. *J. Water Resour. Plan. Manag.* **2002**, *128*, 441–450. [[CrossRef](#)]
- Colombo, A.F.; Karney, B.W. Impacts of Leaks on Energy Consumption in Pumped Systems with Storage. *J. Water Resour. Plan. Manag.* **2005**, *131*, 146–155. [[CrossRef](#)]
- Bylka, J.; Mroz, T. A Review of Energy Assessment Methodology for Water Supply Systems. *Energies* **2019**, *12*, 4599. [[CrossRef](#)]
- Cabrera, E.; Pardo, M.A.; Cobacho, R. Energy Audit of Water Networks. *J. Water Resour. Plan. Manag.* **2010**, *136*, 669–677. [[CrossRef](#)]
- Cabrera, E.; Cobacho, R.; Soriano, J. Towards an Energy Labelling of Pressurized Water Networks. *Procedia Eng.* **2014**, *70*, 209–217. [[CrossRef](#)]
- Cabrera, E.; Gomez, E.; Cabrera, E., Jr.; Soriano, J. Calculating the Economic Level of Friction in Pressurized Water Systems. *Water* **2018**, *10*, 763. [[CrossRef](#)]
- Cabrera, E.; Gómez, E.; Soriano, J.; Del Teso, R. Eco-Layouts in Water Distribution Systems. *J. Water Resour. Plan. Manag.* **2019**, *145*, 04018088. [[CrossRef](#)]
- Cabrera, E.; Gomez, E.; Soriano, J.; Espert, V. Energy Assessment of Pressurized Water Systems. *J. Water Resour. Plan. Manag.* **2015**, *141*, 04014095. [[CrossRef](#)]
- Gomez, E.; Cabrera, E.; Balaguer, M.; Soriano, J. Direct and Indirect Water Supply: An Energy Assessment. *Procedia Eng.* **2015**, *119*, 1088–1097. [[CrossRef](#)]
- Hashemi, S.; Filion, Y.R.; Speight, V.L. Pipe-level Energy Metrics for Energy Assessment in Water Distribution Networks. *Procedia Eng.* **2015**, *119*, 139–147. [[CrossRef](#)]
- Sarbu, I. A Study of Energy Optimisation of Urban Water Distribution Systems Using Potential Elements. *Water* **2016**, *8*, 593. [[CrossRef](#)]
- Gómez, E.; Del Teso, R.; Cabrera, E.; Cabrera, J.E.; Soriano, J. Labeling Water Transport Efficiencies. *Water* **2018**, *10*, 935. [[CrossRef](#)]
- Mamade, A.; Sousa, C.; Marques, A.; Loureiro, D.; Alegre, H.; Covas, D. Energy Auditing as a Tool for Outlining Major Inefficiencies: Results from a Real Water Supply System. *Procedia Eng.* **2015**, *119*, 1098–1108. [[CrossRef](#)]
- Mamade, A.; Loureiro, D.; Alegre, H.; Covas, D. A comprehensive and well tested energy balance for water supply systems. *Urban Water J.* **2017**, *14*, 853–861. [[CrossRef](#)]
- Mamade, A.; Loureiro, D.; Alegre, H.; Covas, D. Top-Down and Bottom-Up Approaches for Water-Energy Balance in Portuguese Supply Systems. *Water* **2018**, *10*, 577. [[CrossRef](#)]
- Cabrera, E.; Del Teso, R.; Gómez, E.; Cabrera, E.; Estruch-Juan, E. Deterministic Model to Estimate the Energy Requirements of Pressurized Water Transport Systems. *Water* **2021**, *13*, 345. [[CrossRef](#)]
- Lenzi, C.; Bragalli, C.; Bolognesi, A.; Artina, S. From energy balance to energy efficiency indicators including water losses. *Water Supply* **2013**, *13*, 889–895. [[CrossRef](#)]
- Dziedzic, R.; Karney, B.W. Energy Metrics for Water Distribution System Assessment: Case Study of the Toronto Network. *J. Water Resour. Plan. Manag.* **2015**, *141*, 04015032. [[CrossRef](#)]
- Wong, H.G.; Speight, V.L.; Filion, Y.R.; Wong, H.G. Impact of Urban Development on Energy Use in a Distribution System. *J. Am. Water Work. Assoc.* **2017**, *109*, E10–E18. [[CrossRef](#)]
- Lappraser, S.; Pornprommin, A.; Lipiwattanakarn, S.; Chittaladakorn, S. Energy Balance of a Trunk Main Network in Bangkok, Thailand. *J. Am. Water Work. Assoc.* **2018**, *110*, E18–E27. [[CrossRef](#)]
- Lipiwattanakarn, S.; Kaewsang, S.; Pornprommin, A.; Wongwiset, T. Real benefits of leak repair and increasing the number of inlets to energy. *Water Pract. Technol.* **2019**, *14*, 714–725. [[CrossRef](#)]
- Alegre, H.; Baptista, J.M.; Cabrera, E.; Cubillo, F.; Duarte, P.; Hirner, W.; Merkel, W.; Parena, R. *Performance Indicators for Water Supply Services*; IWA Publishing: London, UK, 2006.
- Rossman, L.A. *EPANET 2 Users Manual, Water Supply and Water Resources Division*; USEPA: Cincinnati, OH, USA, 2000.